

On the turbulent α -disks and the intermittent activity in AGN

Agnieszka Janiuk and Bożena Czerny

Nicolaus Copernicus Astronomical Center, Bartycka 18, 00-716 Warsaw, Poland

agnes@camk.edu.pl, bcz@camk.edu.pl

Aneta Siemiginowska

Harvard-Smithsonian Center for Astrophysics, 60 Garden Street, MA02138, Cambridge, USA

asiemiginowska@cfa.harvard.edu

Ryszard Szczerba

Nicolaus Copernicus Astronomical Center, Rabiniańska 8, 87-100 Toruń, Poland

szczerba@ncac.torun.pl

ABSTRACT

We consider effects of the MHD turbulence on the viscosity during the evolution of the thermal-viscous ionization instability in the standard α -accretion disks. We consider the possibility that the accretion onto a supermassive black hole proceeds through an outer standard accretion disk and inner, radiatively inefficient and advection dominated flow. In this scenario we follow the time evolution of the accretion disk in which the viscosity parameter α is constant throughout the whole instability cycle, as implied by the strength of MHD turbulence. We conclude that the hydrogen ionization instability is a promising mechanism to explain the intermittent activity in AGN.

Subject headings: accretion, accretion disks – black hole physics – galaxies: evolution

1. Introduction

The standard accretion disk (Shakura & Sunyaev 1973) is known to be subject to the thermal-viscous instability due to the partial hydrogen ionization (Meyer & Meyer-Hofmeister 1981; Smak 1984). As a result of this instability the disk cycles between the two states: a hot and mostly ionized state with a large local accretion rate and a cold, neutral state with a low accretion rate. This instability has originally been proposed to explain the large amplitude luminosity variations observed in cataclysmic variables (CV; Smak 1982; Meyer & Meyer-Hofmeister 1982). It is also believed that the same mechanism is responsible for the eruptions in soft X-ray transients (SXT; see e.g. Cannizzo, Ghosh & Wheeler 1982; Dubus, Hameury & Lasota 2001; Lasota 2001 for review). The ioniza-

tion instability was also shown to operate in the disk around a supermassive black hole in active galactic nuclei (AGN; Lin & Shields 1986; Clarke 1988; Mineshige & Shields 1990; Siemiginowska, Czerny & Kostyunin 1996).

The characteristic timescales of a cycle activity scale roughly with the mass of a compact object (Hatziminaoglou et al. 2001). Therefore, the observed timescale of cycle of order of years in binaries translates into thousands to millions of years in galaxies, which harbor a supermassive black hole.

The variability amplitudes and timescales observed in Galactic binary systems require the viscosity to be smaller in the quiescent disk than during the outburst. Various *ad-hoc* viscosity scaling laws have been used in the disk evolution models,

including the simplest one with a constant viscosity, however usually α is assumed to be 4-5 times larger during the outburst than in the quiescence (Cannizzo 1993). The value of α_{hot} determines the timescale of an outburst, while α_{cold} governs the separation between the subsequent outbursts. The difference between these two parameters determines the outburst amplitude.

The dependence of the viscosity parameter on the disk state is suggested to come out as a property of the magneto-rotational instability (MRI) mechanism (Balbus & Hawley 1991; 1998). Non-linear development of this instability, which is assumed to be a primary source of the disk turbulence, is sensitive to the presence of resistive diffusion of magnetic field (Hawley, Gammie & Balbus 1996), measured by the magnetic Reynolds number Re_M . Gammie & Menou (1998) calculated the Reynolds number for the two states of the disk in CVs and show that it is low in the quiescence. It means that the magneto-hydrodynamical (MHD) turbulence dies away and the matter accumulates in the outer disk.

Menou & Quataert (2001) argued that the Reynolds number will not be low enough to suppress the MHD turbulence in the quiescent disk of AGN. Therefore the efficiency of angular momentum transport should be comparable in the hot and cold states ($\alpha_{\text{cold}} \approx \alpha_{\text{hot}}$). In such a case the outburst amplitude is dramatically reduced, and the ionization instability leads only to a small amplitude flickering (Siemiginowska et al. 1996).

The conclusion about the small amplitude of outbursts was obtained, however, for a geometrically thin, optically thick disk extending down to the marginally stable orbit. This assumption may not be correct. When the local accretion rate is low, the local radiative cooling may not be efficient (Rees et al. 1982; Begelman 1985). The innermost part of the disk may be replaced with an optically thin, hot and possibly two-temperature plasma. An example of such a solution, advection dominated accretion flow (ADAF) was introduced by Ichimaru (1977) and Narayan & Yi (1994). The development of the inner flow through the disk evaporation was recently discussed by several authors, starting with Meyer & Meyer-Hofmeister (1994).

In this paper we first perform a self-consistency check of the α description of the angular momen-

tum transfer. Having justified $\alpha_{\text{cold}} = \alpha_{\text{hot}}$ approach to AGN accretion disks, we consider the time evolution of the disk under the influence of the ionization instability. We also take into account the evaporation of the inner disk.

We define a parameter space where the instability zone (i.e. the partial hydrogen ionization zone) and the evaporation region overlap. The overlapping of these two regions strongly enhances the outburst amplitude due to the time evolution of the disk evaporation radius. We illustrate this behavior with exemplary lightcurves.

The structure of this article is as follows. In Section 2 we define the criterion for efficient development of the MHD turbulence in the accretion disk, taking into account its vertical structure. We confirm that indeed the bi-modal viscosity behavior is characteristic for Galactic binary systems. However, a single value of the viscosity parameter is appropriate in the case of AGN disks. In Section 3 we check if the zone of partial hydrogen ionization overlaps with the disk evaporation region and we calculate the evolution of the disk luminosity in case of the evaporated inner disk. Finally, in Section 4 we discuss our results and give conclusions.

2. Magneto-rotational turbulence

In this Section we estimate the strength of the MHD turbulence in the α accretion disks and investigate whether the viscosity prescription with a constant parameter α is appropriate for both Galactic systems (CVs and SXTs) and AGN. We only consider the instability due to partially ionized hydrogen and do not include regions affected by the radiation pressure instability (see Janiuk, Czerny & Siemiginowska 2002 for that model details). We assume that the viscous stress tensor is proportional to the gas pressure P_{gas} and therefore there is no radiation pressure dominated branch on the stability figures (so-called S-curves) described below.

We use the dimensionless accretion rate in Eddington units, $\dot{m} = \dot{M}/\dot{M}_{\text{Edd}}$, assuming the efficiency of 1/12, as implied for the Schwarzschild black hole by the Newtonian potential:

$$\dot{M}_{\text{Edd}} = 3.52 \frac{M}{10^8 M_{\odot}} [M_{\odot}/yr]. \quad (1)$$

The disk vertical structure (indicated by z) is calculated by solving the equations of viscous energy dissipation, hydrostatic equilibrium, and energy transfer:

$$\frac{dF}{dz} = \alpha P_{\text{gas}} \left(-\frac{d\Omega}{dr} \right) \quad (2)$$

$$\frac{1}{\rho} \frac{dP}{dz} = -\Omega^2 z \quad (3)$$

$$\frac{dT}{dz} = -\frac{3\kappa\rho}{4acT^3} F_1 \quad (4)$$

where we solve for temperature, density and pressure profiles, $T(z)$, $\rho(z)$ and $P(z)$. Here Ω is the Keplerian angular velocity, a and c are physical constants. F_1 is the energy flux transported locally in the direction perpendicular to the equatorial plane and carried either by radiation or by convection:

$$F_1 = F_{\text{rad}} \quad \nabla_{\text{rad}} \leq \nabla_{\text{ad}}, \quad F_1 = F_{\text{rad}} + F_{\text{conv}} \quad \nabla_{\text{rad}} > \nabla_{\text{ad}} \quad (5)$$

The frequency-averaged opacity κ is taken to be the Rosseland mean and includes the electron scattering, free-free and bound-free transitions. The opacity tables are from Alexander, Johnson & Rypma (1983) and Seaton et al. (1994). The presence of dust and molecules is included in the opacity description. The details of the model were discussed in Pojmański (1986) and Różańska et al. (1999).

Figures 1 and 2 show, in Σ vs. T_{eff} (surface density vs. effective temperature) plane, the local solutions of the disk vertical structure calculated for a range of accretion rates for two extreme cases of the mass of the central object: $1M_{\odot}$ and $3 \times 10^9 M_{\odot}$. The solutions located on both lower (below point A) and upper (above point B) branches of the S-curves are stable. The slope of the middle branch is, at least in some parts, negative which means that at that range of accretion rates the disk is thermally and viscously unstable.

Note, that in case of CVs (Figure 1) the location of the starting point of the instability is very sensitive to the adopted value of α . For a small viscosity parameter, $\alpha = 0.02$, the point A is at much lower temperature than in case of large $\alpha = 0.1$. The latter 'smoothens' the S-curve in its lower part, so that only a single 'wiggle' remains. Therefore the point A, defined as the first critical

point above which the S-curve slope becomes negative, is shifted upwards in temperature in comparison with that characteristic for small viscosities. This fact should be taken into account when modeling the limit cycle in dwarf novae by means of the 'combined' S-curves with $\alpha_{\text{cold}} < \alpha_{\text{hot}}$.

This behavior is however characteristic only for accretion disks around $1M_{\odot}$, while vanishes already for SXTs. Also for supermassive black holes there are always two 'wiggles' in the S-curve, regardless of the viscosity parameter.

The ionization instability is characteristic for all accretion disks but the range of accretion rates (i.e. the location of the S-curve on the $T-\Sigma$ plane) depends on the chosen disk radius. We can invert this problem and say that for a fixed external accretion rates the instability will appear only for a certain range of radii. At larger radii the disk is on the lower stable branch while at lower radii it is on the higher, also stable branch. Simple analytical formulae for the unstable zone were provided by Siemiginowska et al. (1996) and applied by Menou & Quataert (2001) in their analysis.

In Figure 3 we show the radial extension of the unstable zone as a function of the accretion rate (in Eddington units) calculated numerically from our disk model. The position of the instability zone depends on the mass of the central object so we choose values representative for all objects from CVs to AGN with a large black hole mass. The plot shows the radial extension as a function of the accretion rate (in Eddington units). The horizontal slices of the shaded region correspond to the accretion rates, for which the disk is unstable at a particular radius. For $\dot{m} \approx 0.01$ (an accretion rate typical for many objects) the instability zone is located at $\sim 10^5 R_{\text{Schw}}$ for a CV, at $\sim 2 \times 10^3 R_{\text{Schw}}$ for $M \sim 10^6 M_{\odot}$ and at $\sim 500 R_{\text{Schw}}$ for an extremely massive black hole of $M = 3 \times 10^9 M_{\odot}$.

Time evolution of the unstable part of the disk proceeds roughly in the form of oscillations between the upper and the lower stable branches. As argued by Gammie & Menou (1998), high temperature upper branch conditions are always favorable for the development of the efficient MRI and high values of viscosity are appropriate there. Lower branch conditions are different and the MRI mechanism may not be efficient. Therefore, we perform our self-consistency check paying particular attention to the lower branch solutions at the

vicinity of the turning point A .

2.1. Coupling of the magnetic field with the gas

The behavior of the magnetic field is governed by the fluid conductivity σ . The time-dependent magnetic field in the disk is described by the equation (Parker 1979):

$$\frac{\partial \vec{B}}{\partial t} = \nabla \times (\vec{v} \times \vec{B}) + \eta \nabla^2 \vec{B} \quad (6)$$

where $\eta \equiv c^2/4\pi\sigma$ denotes resistivity. The characteristic diffusion time in which the initial configuration of the magnetic field will decay is equal to $\tau = L^2/\eta$, where L indicates the characteristic spatial scale. For timescales short in comparison with τ the second term in Equation 6 can be neglected and the magnetic field lines are frozen into the gas. Magnetic Reynolds number, defined as:

$$Re_M = \frac{v\tau}{L} \quad (7)$$

can be used to distinguish between two cases: (1) the diffusion of field lines within the disk and (2) the lines are frozen in and carried along with the matter. Here we identify the velocity v with the sound speed in the disk and the length L of the magnetic field spatial variations with the disk thickness, as commonly used in the simulations (see e.g. Hawley et al. 1996; Gammie & Menou 1998).

Apart from the ohmic diffusion also the ambipolar diffusion may be important. The ambipolar Reynolds number is defined as:

$$Re_A = \frac{\nu_{ni}}{\Omega} \quad (8)$$

where ν_{ni} is the frequency of collisions between ions and neutral particles.

We can calculate the both Reynolds numbers locally in the disk. In order to determine the resistivity, $\eta = (c^2 m_e / 4\pi e^2) \times (\nu_{en} / n_e)$, we have to estimate the number density of electrons n_e and neutral particles n_n . The frequency of collisions between electron and neutral particles is defined as $\nu_{en} = 8.3 \times 10^{-10} T^{1/2} n_n$ in s^{-1} (Draine, Roberge & Dalgarno 1983). The ionization fraction $x_e = n_e / n_n$ is calculated from the Saha equation for any given value of temperature and density in the disk. In this temperature range the

free electrons originate mostly from the ionization of hydrogen, sodium, potassium and calcium.

The magneto-rotational instability acts over the entire disk thickness. Therefore, we need to consider the entire vertical disk structure when we estimate the coupling of the magnetic field to the gas. This is why instead of calculating Re_A and Re_M at the equatorial plane, we introduce the density weighted values of these parameters, integrated over the disk height:

$$\bar{Re}_A = \frac{\int_0^H Re_A \rho(z) dz}{\int_0^H \rho dz} \quad (9)$$

and

$$\bar{Re}_M = \frac{\int_0^H Re_M \rho(z) dz}{\int_0^H \rho dz} \quad (10)$$

where $\rho(z)$ is the density profile determined from the vertical structure model and $H \equiv z_{\max}$ is the disk thickness.

Numerical simulations (Hawley et al. 1996; Hawley & Stone 1998) show that below the critical Reynolds numbers (defined as in Equations 7 and 8):

$$Re_M^{\text{crit}} = 10^4 \quad (11)$$

and

$$Re_A^{\text{crit}} = 100 \quad (12)$$

the action of MHD turbulence is inefficient and cannot be important in the angular momentum transport in the disk. As a consequence, the viscosity parameter ($\alpha \approx \alpha_{\text{mag}}$) is very small.

If the disk Reynolds numbers drop below critical values in the quiescence (e.g. on the lower branch of the S-curve), while rise above the critical values in the outburst (e.g. on the upper branch of the S-curve) then the assumption that $\alpha_{\text{cold}} \ll \alpha_{\text{hot}}$ (see Figure 1) is justified. Otherwise, the viscosity parameter should be the same on both cold and hot branches of the S-curve (see Figure 2). Below we calculate the Reynolds numbers in the quiescent disk and test them against the critical values in different types of accreting systems.

2.2. Results

2.2.1. Accretion disks in binary systems

We consider an accretion disk in CVs, e.g. around a white dwarf with a mass $M=1M_{\odot}$ and

calculate the disk vertical structure at two exemplary radii: $10^4 R_{\text{Schw}}$ and $10^5 R_{\text{Schw}}$. Figure 4 (a) shows the magnetic and ambipolar Reynolds numbers for the case of small viscosity parameter $\alpha = 0.02$. It is plotted as a function of the accretion rate corresponding to the lower branch of the S-curve (e.g. in Figure 1 below the point *A*). Point *A* indicates the highest accretion rate on the lower, stable branch of the S-curve. Both Reynolds numbers are below the critical values for most part of the lower branch. Magnetic Reynolds number is somewhat above the critical value close to the point *A*. The ambipolar Reynolds number is well below the critical value at the smallest radius and approaches it at the point *A* only for the largest radius. In general, the magnetic number at the lower branch is almost independent from the radius. The ambipolar number is increasing with the radius. However, the value of $10^5 R_{\text{Schw}}$ is rather an upper limit for the disk size in CV systems so any values of the Reynolds number larger than those in Figure 4 are not expected.

In Figure 4 (b) we plot the magnetic and ambipolar Reynolds numbers up to the point *A* for large value of $\alpha = 0.1$. In this case the Reynolds numbers are mostly small, but as the point *A* reaches this time higher temperatures, also their values can exceed critical ones in the end of the extended stable branch.

Therefore, whenever the viscosity drops at the lower branch it will have a tendency to remain low. This result supports the view that the angular momentum transport due to MHD turbulence cannot be efficient when the disk is in the quiescence and the assumption that $\alpha_{\text{cold}} \ll \alpha_{\text{hot}}$ is justified.

We obtain a similar result for black hole X-ray transient systems with $M_{\text{BH}} \sim 10 M_{\odot}$ as shown in Figure 5. The calculated magnetic and ambipolar Reynolds numbers fall generally below the critical values for the quiescent disk in these systems, regarding also the fact that this time there is no difference in the location of the point *A* caused by the change in α .

2.2.2. AGN accretion disks

Now we consider accretion disks in AGN, e.g. systems harboring a supermassive black hole. Note, that for an accretion disk around a supermassive black hole the temperatures are lower

than in the stellar mass black hole case. Therefore the ionization instability zone is located much closer to the central black hole and in our calculations we have to consider radii of order of a few hundreds R_{Schw} instead of hundreds of thousands.

We calculate the Reynolds numbers for a range of masses between $10^6 M_{\odot}$ and $3 \times 10^9 M_{\odot}$. We found that the Reynolds numbers are orders of magnitude above the critical values, for the most part of the lower branch, and the greater the mass of a black hole, the larger Re . In Figure 6 we plot magnetic and ambipolar Reynolds numbers as a function of the accretion rate corresponding to the lower, cold branch of the S-curve for $3 \times 10^9 M_{\odot}$.

Both Reynolds numbers clearly exceed the critical values: 10^2 and 10^4 for Re_A and Re_M respectively. Therefore only for very low accretion rates, $\dot{m} < 10^{-4}$, MHD turbulence in the disk would not develop and practically the entire cold branch of the S-curve is MHD turbulent. This result only weakly depends on the adopted viscosity parameter value. For $\alpha = 0.02$ both Reynolds numbers had similar values to these presented in Figure 6 and were always greater than critical ($\bar{Re}_M > 10^6$ and $\bar{Re}_A > 10^5$ at the disk radius of $\log R = 16.5$ [cm]).

In order to understand whether the above result is valid for the entire disk we calculate the Reynolds numbers at different locations in the following way. At each radius we compute the entire S-curve, such as that in Figure 2, determine the position of the turning point *A* and calculate the Reynolds numbers $\bar{Re}_A(A)$ and $\bar{Re}_M(A)$ at this point. Their values measured along the lower branch of the S-curve are lower (equal) to $\bar{Re}_A(A)$ and $\bar{Re}_M(A)$. We summarize this result in Figure 7, plotting the Reynolds numbers against the radius. Both \bar{Re}_A and \bar{Re}_M increase with radius implying that MRI is stronger further out in the disk. They decrease towards smaller radii but do not drop below the critical values even at $10 R_{\text{Schw}}$.

Our results support the view presented in Menou & Quataert (2001) and imply that in the thermally unstable AGN disks the viscosity should not change between the cold and hot states of the disk (i.e. $\alpha_{\text{cold}} = \alpha_{\text{hot}}$).

3. Evaporation of the disk

We concluded above that the viscosity parameter in AGN accretion disks does not vary between the cold and hot states of the disk. As a result the ionization instability will cause only small amplitude luminosity fluctuations not really detectable in the observations (Siemiginowska, Czerny & Kostyunin 1996; Menou & Quataert 2001). However, variations in the local accretion rate induced by the instability may result in the disk evaporation and affect the disk luminosity (Siemiginowska 1998). Here, we investigate the effects of the disk evaporation on the overall evolution of thermally unstable disk. We assume that $\alpha_{\text{cold}} = \alpha_{\text{hot}} = 0.1$.

3.1. Evaporation radius

The accretion flow in low luminosity systems can occur either via a standard cold disk or via an advection dominated flow (ADAF). In the latter the bulk of gravitational energy is advected into the central object instead of being radiated (Ichimaru 1977; Narayan & Yi 1994). The ADAF solution forms below a certain transition radius that depends on the accretion rate. In classical ADAF model (Abramowicz et al. 1995; Honma 1996; Kato & Nakamura 1998) this relation is:

$$R_{\text{evap}} = 1.9\dot{m}^{-2}\alpha_{0.1}^4 R_{\text{Schw}}. \quad (13)$$

The transition radius between the outer disk and inner ADAF was discussed in several papers (e.g. Liu et al. 1999; Rózańska & Czerny 2000; Menou et al. 2000; Liu et al. 2002; Meyer & Meyer-Hofmeister 2002), under various assumptions. Here we adopt the canonical approach.

The ionization instability can develop only when the standard thin disk reaches the temperatures sufficient for the hydrogen ionization. If accretion rates are low the disk can evaporate without being ionized (e.g. without reaching point *A* on the stability S-curve) and the instability does not develop. Therefore the evaporation radius cannot be very large for the ionization to occur:

$$R_{\text{evap}} < R_{\text{instab}}. \quad (14)$$

In Figure 3 we showed the radial extension of the unstable ionization zone as a function of the accretion rate. The instability cycle operates between the points *A* and *B* of the S-curve (cf. Figure 2), so we consider this entire range of accretion

rates to be unstable. In Figure 3 we also indicate a location of R_{evap} for the ADAF prescription (note, that the evaporation radius does not depend on mass of a black hole). If the disk evaporates, only the unstable region *above* the solid line may exist and contribute to the total disk luminosity. The extension of the unstable region does not depend on α very much, while the formula defining the evaporation radius strongly depends on it. Therefore, we should emphasize that our result may be very sensitive to the adopted value of the viscosity parameter. Possibly, depending on α , the entire unstable region of the disk evaporates, or, on the other hand, the evaporation radius is very small and does not affect the instability.

Because the location of the evaporation radius depends on viscosity, if it can be determined observationally it may provide a new method of estimating the value of the α parameter in accreting objects. For example, recently Nayakshin & Sunyaev (2003) proposed a new model explaining the X-ray flares in the Galactic Center by the star-disk interactions. This model would favor the case of the disk extending quite close to the central black hole. However, the presence of the disk in the Galactic Center is still unclear (see Quataert 2003 for a review).

3.2. Luminosity of the disk with inner ADAF

Below we study the evolution of the disk affected by the ionization instability assuming that the viscosity parameter is constant, as favored for accreting supermassive black holes. We used the method described in Siemiginowska, Czerny & Kostyunin (1996) and consider the two cases: (i) the accretion disk extends down to the marginally stable orbit and (ii) the central part of the disk is evaporated and forms an ADAF, while the standard thick disk remains at the outer radii. Since the accretion efficiency of an ADAF is low, we assume that this part of the flow does not contribute to the luminosity.

In order to determine the disk evaporation radius during the evolution we compare the local accretion rate with the critical (evaporation) accretion rate. We use the classical ADAF prescription, expressed by Equation 13. In Figure 8 we show radial profiles of the local accretion rate in several snapshots during one cycle of the disk in-

stability. The straight solid line marks the critical accretion rate. Whenever the local accretion rate in the disk drops below this critical value, the disk evaporates and ADAF is formed. Hereafter, in our time dependent calculations we assume that the ADAF transition radius is the outermost radius at which the disk evaporates. Therefore even though the local accretion rate may be equal to the critical value at several locations in the disk, only the outermost one determines the transition radius and the standard disk cannot rebuilt itself below this radius.

In Figure 9 we present lightcurves for the two models: (i) the standard disk and (ii) the disk with inner ADAF. When the disk extends all the way to the marginally stable orbit, as considered in the previous time-dependent calculations, the luminosity variations are small and only a small flickering ($\Delta \log L_{\text{disk}} \sim 0.2$) can be seen in the resulting lightcurve. This is indicated by the upper solid line in Figure 9.

However, the situation changes dramatically, when the evaporation of the inner disk is taken into account. In this case the ionization instability leads to strong, large-amplitude outbursts. These outbursts are due to the large variations of the inner radius of the accretion disk (e.g. the size of the ADAF), as determined by the critical value of the local accretion rate. The outburst peak corresponds to the moment, when the inner disk radius is small and the entire accretion disk contributes to the total luminosity. The quiescent low luminosity state, on the other hand, is achieved when the local accretion rate drops below the critical value at the large distance from the center and most of the inner disk is evaporated.

4. Discussion and conclusions

We studied the effects of MHD turbulence and the efficiency of angular momentum transport in the quiescent accretion disks. We analyzed the full disk vertical structure, which enabled us to determine accurately the coupling of the accreting gas to the magnetic field over the entire disk height.

Confirming the previous results of Menou & Quataert (2001), we find that only in the case of accretion disks in binary systems, e.g. around white dwarfs (CVs) or stellar mass black holes (SXTs), the timescale of the magnetic field de-

cay is too short for the field to be frozen into the gas. Therefore, MHD turbulence does not operate efficiently and the large amplitude outbursts observed in these sources can be accounted for by the thermal ionization instability cycle in which $\alpha_{\text{cold}} \ll \alpha_{\text{hot}}$. On the other hand, in the case of accreting supermassive black holes in AGN the gas in the disk is well coupled to the magnetic field.

This effect ($Re_M \gg 1$ and $Re_A \gg 1$) can be only slightly reduced by encounters of free electrons with charged dust particles. In principle, the presence of dust in the disk can affect the number density of free electrons. However, the grains evaporate if the temperature exceeds $\sim 1800 - 2000$ K, which is the case near the disk equatorial plane. As a result, the role of the dust in suppressing MHD turbulence is limited only to the uppermost disk layers and cannot have a global effect. We conclude, that the AGN accretion disks in quiescence have comparable angular momentum transport efficiency to the disks in outburst.

Therefore, we studied the ionization instability assuming a constant value of the viscosity parameter $\alpha_{\text{cold}} = \alpha_{\text{hot}}$. We took into account the evaporation of the innermost parts of the disk during the quiescence in AGN accretion disks. The transition to an ADAF below the evaporation radius during the evolution of the instability results in large luminosity variations ($\Delta \log L_{\text{disk}} \sim 2$). Because only the outer parts of the disk ($R > R_{\text{evap}} \sim 10^3 R_{\text{Schw}}$) contribute to the total disk emission the minimum luminosity obtained within the instability cycle is lower than in the standard disk with no evaporation. We note, that also during the outburst the evaporation is important and ADAF remains in the innermost regions of the disk ($R_{\text{evap}} \sim 25 R_{\text{Schw}}$), even at quite a high global accretion rate, $\dot{M} = 0.1 \dot{M}_{\text{Edd}}$. The evaporation radius, however, strongly depends on the adopted value of the viscosity parameter α (cf. Equation 13).

The α -disks in AGN are self-gravitating beyond a certain radius (Paczynski 1978; Hure 1998). A typical distance of the self-gravitating zone is about a thousand Schwarzschild radii (Hure 2000). However, the greater the black hole mass and lower the parameter α , the closer to the center this zone is located. We can include a self-gravitation term equal to $-4\pi G\Sigma$ in Equation 3 of the disk vertical structure. This additional term modi-

fies the S-curve, so there is a single 'wiggle' on the middle branch of the curve, instead of two. The middle branch is also broader and reaches lower surface densities. The instability happens for a narrower range of effective temperatures, while the more strongly curved unstable middle branch covers broader range of surface density values. Therefore, the amplitude of the outburst is not expected to be significantly modified in our model by the presence of self-gravity. However, whether the model actually can be extended into the self-gravity region, remains an open question. In particular, our description of convection, which influences the shape of the S-curve, may not be applicable in case of a self-gravitating disk. Also, MRI was not extensively studied in the self gravity region (but see Fromang et al. 2003) and the use of viscosity parameter α may not be appropriate here. Instead, self-gravity may either provide a mechanism of angular momentum transfer (e.g. Paczyński 1978), or lead to the disk fragmentation and star formation (Collin & Zahn 1999). The physics of those processes is poorly known. Therefore the use of simple models like α -disks and comparison of their predictions with observed behavior of AGN seems to be justified.

The variability amplitudes predicted by our model are about two orders of magnitude and support the observational evidence of intermittent activity of AGN. This kind of activity has been proposed to explain the formation of giant radio galaxies (Subrahmanyam et al. 1996) and the extended radio structures in the Giga-Hertz Peaked Spectrum (GPS) radio sources (Baum et al. 1990; Schoenmakers et al. 1998). The timescales of episodic activity in quasars were recently estimated by Martini & Schneider (2003). Recent observations of Compact Steep Spectrum (CSS) sources indicate that the evolutionary path of radio loud AGN is consistent with an on-off activity with duration governed by the mass of the central black hole (Marecki et al. 2003). Also the black hole masses implied by the HST observations of normal galaxies and AGN suggest that every galaxy must undergo an active phase in its life (Ferrarese et al. 2001).

The estimated timescales of the activity cycle are within 10^5 to 10^7 years (e.g. Reynolds & Begelman 1997 for GPS sources). Di Matteo et al. (2003) proposed a feedback mechanism to ex-

plain the cyclic activity in M87, which occurs on a timescale of 10^7 years. In our time-dependent calculations, we adopted a simplified approach to the disk evaporation process, and therefore underestimated the repetition timescale. This is because we do not consider the time of the disk reconstruction after it has been evaporated, which increases the viscous timescale by a factor of ~ 2 . Assuming that the outburst starts at the outer edge of the instability zone we obtain the viscous timescale of $t_{\text{visc}} = 1/(\alpha\Omega) \times (r/H)^2 \approx 0.9$ Myrs for $M_{\text{BH}} = 10^8 M_{\odot}$. Thus the outbursts will be less frequent than these presented in Figure 9. However, because during the outburst there is no ADAF and the entire disk is present, the decay timescale is calculated properly and the duration of an outburst is correct. On the other hand, the outburst profiles will be less steep than the ones calculated here, since the disk density rises gradually at the beginning of the instability cycle. Although these two effects are important, the extension of the unstable region is not very large in comparison with the disk size and the uncertainty involved in our calculations is not crucial. The detailed model of the time evolution of the accretion disk with transition to ADAF is clearly worth investigating and we address it to the future work.

Acknowledgments AJ is grateful to F. Meyer and E. Meyer-Hofmeister for interesting discussion. This work was supported in part by grants 2P03D00322 and 2P03D00124 of the Polish State Committee for Scientific Research. Partial support for this work was provided by the National Aeronautics and Space Administration through Chandra Award Number GO-01164X issued by the Chandra X-Ray Observatory Center, which is operated by the Smithsonian Astrophysical Observatory for and on behalf of NASA under contract NAS8-39073.

References

- Abramowicz M.A., Chen X., Kato S., Lasota J.-P., Regev O., 1995, ApJ, **438**, L37
- Alexander D.R., Johnson H.R., Rypma R.L., 1983, ApJ, **272**, 773
- Balbus S.A., Hawley J.F., 1991, ApJ, **376**, 214
- Balbus S.A., Hawley J.F., 1998, Accretion Processes in Astrophysical Systems: Some Like it Hot!, eds. Holt S.S. & Kallman

- T.R., AIP Conf. Proceedings, **431**, p. 79
- Baum S.A., O’Dea C.P., de Bruyn A.G., Murphy D.W., 1990, A&A, **232**, 19
- Begelman M.C., 1985, Astrophysics of Active Galaxies and Quasi-Stellar Objects, p. 411 (Mill Valley: University Science Books)
- Cannizzo J.K., Ghosh P., Wheeler J.C., 1982, ApJ, **260**, L83
- Cannizzo J.K., 1993, ApJ, **419**, 318
- Clarke C.J., 1988, MNRAS, **235**, 881
- Collin S., Zahn J.-P., 1999, A&A, **344**, 433
- Di Matteo T., Allen S.W., Fabian A.C., Wilson A.S., Young A.J., 2003, ApJ, **582**, 133
- Dubus G., Hameury J.-M., Lasota J.-P., 2001, A&A, **373**, 251
- Ferrarese L., Pogge R.W., Peterson B.M., Merritt D., Wandel A., Joseph C.L., 2001, ApJ, **555**, L79
- Fromang S., de Villiers J.P., Balbus S.A., 2003 (astro-ph/0309816)
- Gammie C.F., Menou K., 1998, ApJ, **492**, L75
- Hatziminaoglou E., Siemiginowska A., Elvis M., 2001, ApJ, **547**, 90
- Hawley J.F., Gammie C.F., Balbus S.A., 1996, ApJ, **464**, 690
- Hawley J.F., Stone J.M., 1998, ApJ, **501**, 758
- Honma F., 1996, PASJ, **48**, 77
- Hure J.-M., 1998, A&A, **337**, 625
- Hure J.-M., 2000, A&A, **358**, 378
- Ichimaru S., 1977, ApJ, **214**, 840
- Janiuk, A., Czerny, B., & Siemiginowska, A., 2002, ApJ, **576**, 908
- Kato S., Nakamura K.E., 1998, PASJ, **50**, 559
- Lasota J.-P., 2001, NewAR, **45**, L449
- Lin D.N.C., Shields G.A., 1986, ApJ, **305**, 28
- Liu B.F., Yuan W., Meyer F., Meyer-Hofmeister E., Xie G.Z., 1999, ApJ, **527**, L17
- Liu B.F., Mineshige S., Meyer F., Meyer-Hofmeister E., Kawaguchi T., 2002, ApJ, **575**, 117
- Marecki A., Spencer R.E., Kunert M., 2003, PASA, **20**, 46
- Martini P., Schneider P., 2003 (astro-ph/0309650)
- Menou K., Hameury J.-M., Lasota J.-P., Narayan R., 2000, MNRAS, **314**, 498
- Menou K., Quataert E., 2001, ApJ, **552**, 204
- Meyer F., Meyer-Hofmeister E., 1981, A&A, **104**, L10
- Meyer F., Meyer-Hofmeister E., 1982, A&A, **106**, 34
- Meyer F., Meyer-Hofmeister E., 1994, A&A, **288**, 175
- Meyer F., Meyer-Hofmeister E., 2002, A&A, **392**, L5
- Mineshige S., Shields G.A., 1990, ApJ, **351**, 47
- Narayan R., Yi L., 1994, ApJ, **428**, L13
- Nayakshin S., Sunyaev R., 2003, MNRAS, **343**, L15
- Parker E.N., 1979, Cosmical Magnetic Fields, (Oxford:Clarendon Press)
- Paczyński B., 1978, Acta Astron., **28**, 91
- Pojmański G., 1986, Acta Astron. **36**, 69
- Quataert, 2003 in Astron. Nachr., Vol. **324**, No. S1 (astro-ph/0304099)
- Rees M.J., Begelman M.C., Blandford R.D., Phinney E.S., 1982, Nature, **295**, 17
- Reynolds C.S., Begelman M.C., 1997, ApJ, **487**, L135
- Rózańska A., Czerny B., Życki P.T., Pojmański G., 1999, MNRAS, **305**, 481
- Rózańska A., Czerny B., 2000, A&A, **360**, 1170
- Schoenmakers A.P., de Bruyn A.G., Rottgering H.J.A., van der Laan H., 1999, A&A, **341**, 44
- Seaton M.J., Yan Y., Mihalas D., Pradhan A.K., 1994, MNRAS, **266**, 805
- Shakura N.I., Sunyaev R.A., 1973, A.&A., **24**, 337
- Siemiginowska A., Czerny B., Kostyunin V., 1996, ApJ, **458**, 491
- Siemiginowska, A. 1998, Accretion Processes in Astrophysical Systems: Some Like it Hot!, eds. Holt S.S. & Kallman T.R., AIP Conference Proceedings **431**, p. 211
- Smak J. 1982, Acta Astron. **32**, 199
- Smak J. 1984, Acta Astron. **34**, 161
- Subrahmanyan R., Saripalli L., Hunstead R.W., 1996, MNRAS, **279**, 257

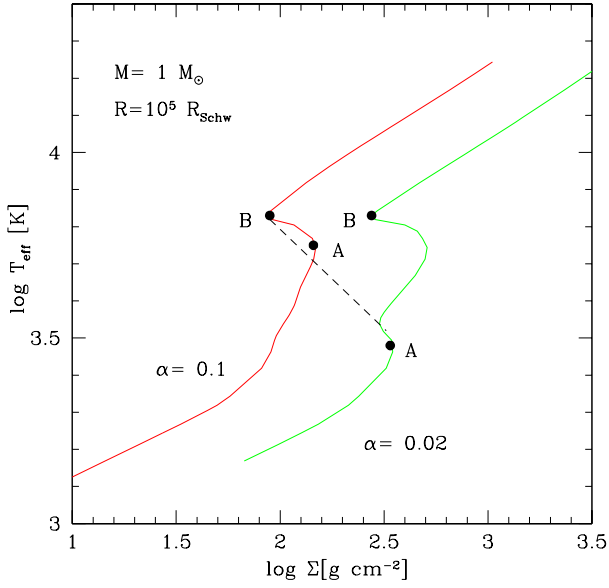


Fig. 1.— The stability curves calculated for the disk around $M = 1M_{\odot}$ at the radius $R = 10^5 R_{\text{Schw}}$. The viscosity parameters are $\alpha = 0.1$ (left curve) and $\alpha = 0.02$ (right curve). The dashed line marks the combined stability curve, which would result from the assumption that $\alpha_{\text{cold}} = 0.02$ (on the lower stable branch) and $\alpha_{\text{hot}} = 0.1$ (on the upper stable branch). Point *A* indicates the lowest location of the unstable disk and a starting point of the ionization instability cycle and the instability ends in the point *B*.

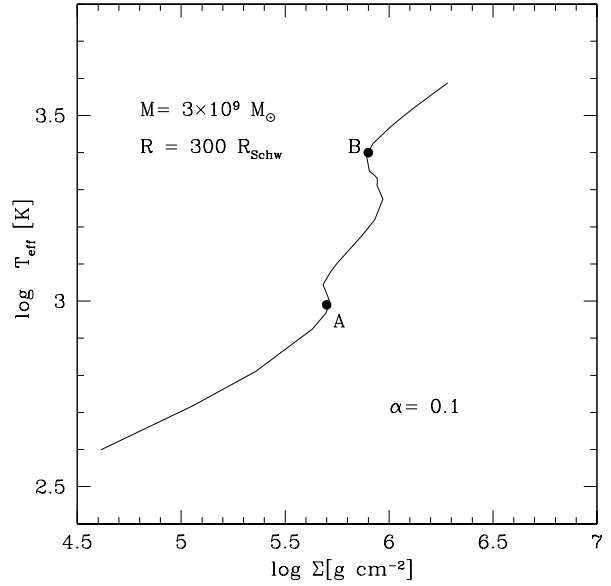


Fig. 2.— The stability curve calculated for the disk around a supermassive black hole of $M = 3 \times 10^9 M_{\odot}$ at the radius $R = 300 R_{\text{Schw}}$. The viscosity parameter is $\alpha = 0.1$. The point *A* is the starting point of the ionization instability cycle and the instability ends in the point *B*.

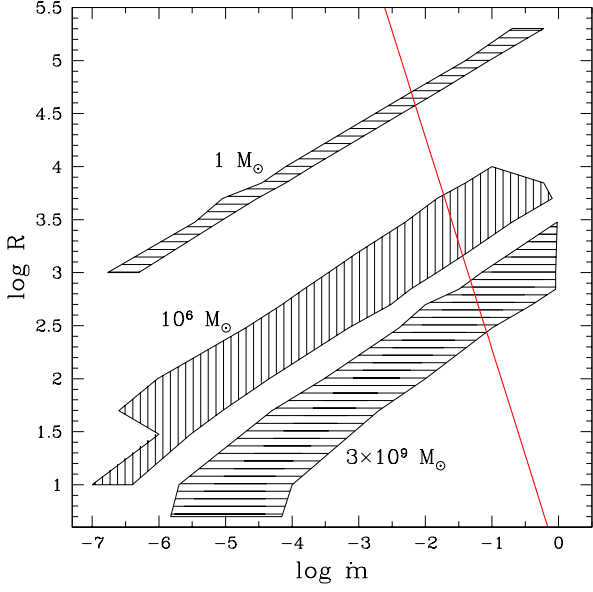


Fig. 3.— The radial extension of the ionization instability zone as a function of the accretion rate. The contours correspond to the turning points A and B on the S-curve (see Figure 2). The thick solid line marks the transition radius, resulting from the ADAF prescription (see text). The black hole mass is $M = 1M_\odot$ (top contour), $M = 10^6 M_\odot$ (middle contour) and $M = 3 \times 10^9 M_\odot$ (bottom contour). The viscosity parameter is $\alpha = 0.1$.

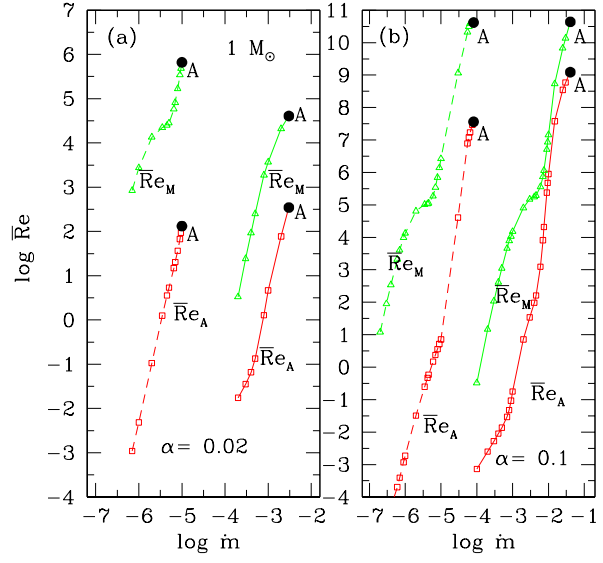


Fig. 4.— The density weighted magnetic and ambipolar Reynolds numbers calculated for the central mass $M = 1M_\odot$, plotted for two disk radii $R = 10^4 R_{\text{Schw}}$ (dashed line) and $R = 10^5 R_{\text{Schw}}$ (solid line), as a function of the accretion rate in the range corresponding to the cold branch of the S-curve (cf. Fig. 1). The viscosity is $\alpha = 0.02$ (panel a) and $\alpha = 0.1$ (panel b).

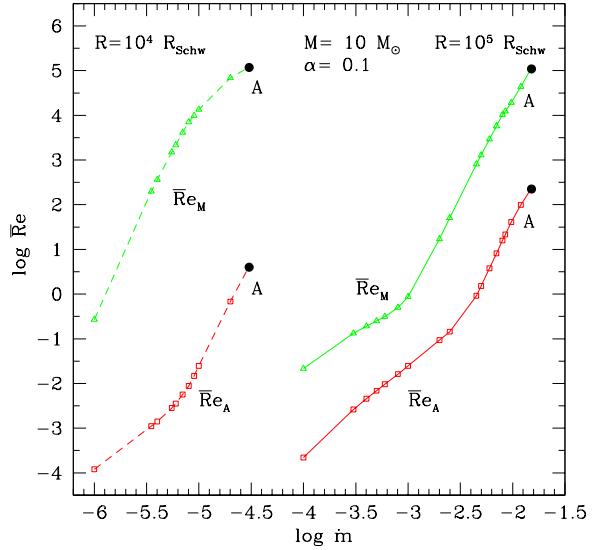


Fig. 5.— The density weighted magnetic and ambipolar Reynolds numbers calculated for black hole mass $M = 10M_\odot$, plotted for two disk radii $R = 10^4 R_{\text{Schw}}$ (dashed line) and $R = 10^5 R_{\text{Schw}}$ (solid line), as a function of the accretion rate in the range corresponding to the cold branch of the S-curve. The viscosity is $\alpha = 0.1$.

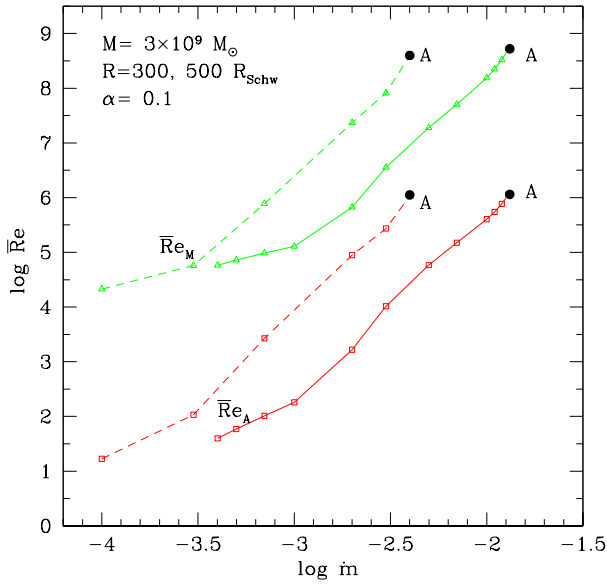


Fig. 6.— The density weighted magnetic and ambipolar Reynolds numbers calculated for black hole mass $M = 3 \times 10^9 M_\odot$, plotted for two disk radii $R = 300 R_{\text{Schw}}$ (dashed line) and $R = 500 R_{\text{Schw}}$ (solid line), as a function of the accretion rate in the range corresponding to the cold branch of the S-curve (cf. Fig. 2). The viscosity is $\alpha = 0.1$.

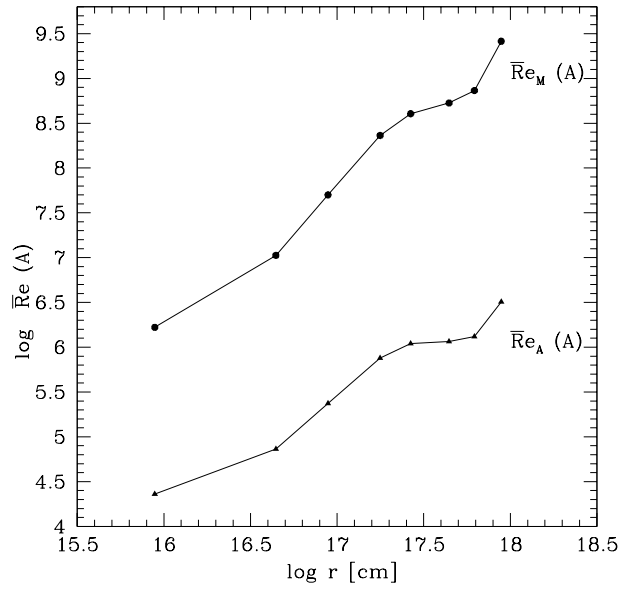


Fig. 7.— The radial profiles of the magnetic (circles) and ambipolar (triangles) Reynolds numbers in the turning point A on the S-curve. The points mark the values obtained for 10, 50, 100, 200, 300, 500, 700 and 1000 R_{Schw} at each curve respectively. The black hole mass is $M = 3 \times 10^9 M_\odot$ and viscosity is $\alpha = 0.1$.

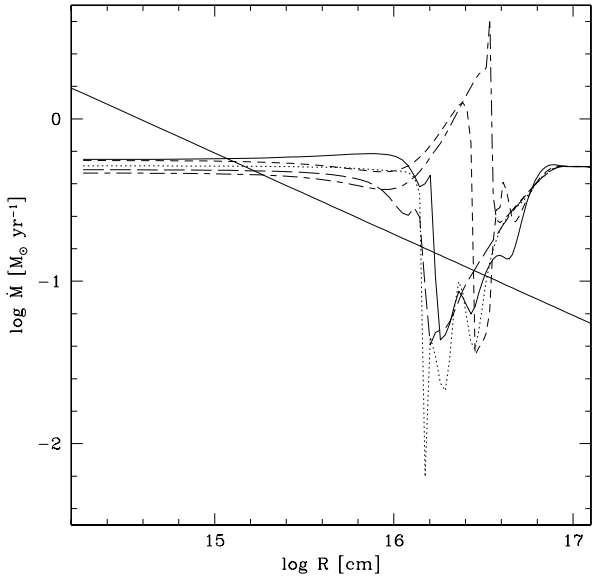


Fig. 8.— The local accretion rate during the cycle of the disk evolution caused by the ionization instability. The thick solid line marks the critical accretion rate, below which the disk is evaporated, resulting from the ADAF prescription (see Eq. 13). The black hole mass is $M = 10^8 M_\odot$ and viscosity $\alpha = 0.1$.

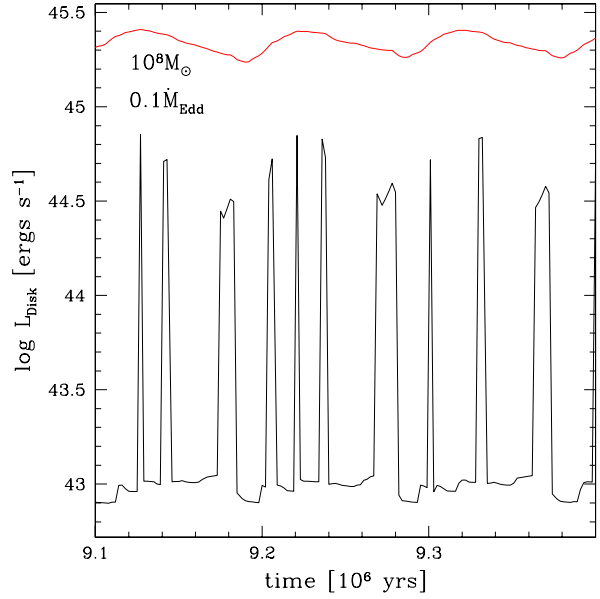


Fig. 9.— The disk lightcurve during the evolution caused by the ionization instability with constant viscosity assumed ($\alpha = 0.1$). The upper curve shows the luminosity flickering resulting from the evolution of the whole disk. The lower curve shows the sharp outbursts of the disk, which inner part is evaporated. The black hole mass is $M = 10^8 M_\odot$ and the global accretion rate is $0.1 \dot{M}_{\text{Edd}}$.